Permanent deformation of bridge abutment on liquefiable soils

Akihiro TAKAHASHI[1], Hideki SUGITA[1] & Shunsuke TANIMOTO[1]

ABSTRACT

Seismic response of a bridge abutment located near a river dyke is the consequence of complex interactions among bridge(s), abutment, foundation ground, embankment, river dyke, and associated lateral spreading of liquefied soils. This paper reports result of preliminary dynamic 3D FE analyses on a bridge abutment constructed adjacent to a river dyke, considering liquefaction of foundation soils, and demonstrates importance of consideration of pile kinematic loading induced by abutment backfill on assessment of seismic response of bridge abutment on liquefiable soils.

1. INTRODUCTION

When seismic performance of a piled road bridge abutment on liquefiable soils is assessed in accordance with the ductility design method adopted in the 2002 Japanese Specifications for Highway Bridges (JRA 2002), we calculate response of the piled abutment subjected to (1) inertia forces of a superstructure and the abutment, and (2) seismic active earth pressure of backfill. In the calculation, liquefaction of foundation soils only contributes to reduce lateral soil resistances in the adjacent soils for simplicity, and no kinematic load induced by interaction between foundation soils and piles is considered. As a result, the current ductility design method could underestimate seismic horizontal displacement of abutment and pile foundation deformation when (1) a height of the abutment is relatively smaller than a thickness of liquefiable soil layer, and/or (2) liquefied ground adjacent to the abutment laterally spreads (Shirato et al., 2005).

We encounter these kinds of situation when a bridge (1) is built on a floodplain or reclaimed area, i.e., liquefiable ground, and (2) crosses river or channel, and especially (3) its abutment is located adjacent to river dyke or revetment, since the river dyke and revetment easily move waterward during an earthquake and cause lateral spreading of soils when their foundation soils are liquefied. Moreover, a road embankment connected to the bridge could be another cause of soil lateral spreading and could make amount of the spreading induced by the river dyke (or revetment) movement larger. As seismic response of bridge abutment on liquefiable soils is the consequence of complex interactions among these, identification of relevant factors that dominate the bridge abutment response for design situation is crucial.

This paper reports result of preliminary dynamic three-dimensional finite element analyses on a bridge abutment constructed adjacent to a river dyke, considering liquefaction of foundation soils, and demonstrates importance of consideration of pile kinematic loading induced by abutment backfill on assessment of seismic response of bridge abutment on liquefiable soils.

[1] Earthquake Disaster Prevention Research Group, Public Works Research Institute, Japan

2. NUMERICAL ANALYSIS CONDITIONS

Target road bridge abutment is a piled abutment constructed in a river dyke. Plan view and cross section of the target abutment are illustrated in Fig. 1. The target bridge crosses a river and distance of two opposed abutments is 70m. The abutment foundation consists of six 2m-cast-in-place concrete piles whose length=20m. The piles are arranged in 2x3 grids having 5m spacing. Width of the bridge is 15m and slope of road embankment connected to the 10m-height piled abutment and river dyke is 1:2. Water level is set to 7.5m below the river dyke crest. The ground level is at a height of 5m above riverbed. Thickness of liquefiable layer (loose sand deposit) below water table is 12.5m and materials of the river dyke and road embankment are assumed the same as that of surface layer above water table. The piles are installed in two layers; a bottom non-liquefiable layer (dense sand deposit) and the liquefiable layer.

In the numerical analysis, only half width of the road bridge in y-direction was modelled taking the advantage of symmetry. Width of the analytical domain in y-direction was 100m, length in x-direction was 240m and depth in z-direction from the riverbed was 20m. Soils, wall and base slab of the abutment were modelled by solid elements and piles were modelled by elastic beam elements whose flexural rigidity was set to that at main reinforcement yielding. The extended subloading surface model proposed by Hashiguchi & Chen (1998) was adopted for the soil layers. Material parameters of the soil layers and the structural components are listed in Table 1, where Gs=specific gravity, e_0=initial void ratio, λ & κ=slopes of compression & swelling lines in v-ln(p') plane, ν=Poisson's ratio, k=hydraulic conductivity, ρ=unit weight, E=Young's modulus, I=flexural rigidity of beam, A=area of beam section, and the other parameters are specific parameters for the constitutive model used. Liquefaction resistance of the non-liquefiable and liquefiable layers is summarised as the cyclic shear stress ratio plotted against the number of loading cycles to cause liquefaction in triaxial tests as shown in Fig. 2.

Movement of x=–40 & 200m planes were set to follow that of the level ground. y=0 & 100m planes were allowed to move freely in the x- and z-directions but not in the y-direction. At the bottom z=–20m plane, all movements were restrained. Fluid flow velocities normal to the analytical domain boundary were set to zero at side and bottom boundaries. Figure 3 shows the applied earthquake motion whose maximum acceleration is 525gal. This was applied in x-direction. In order to obtain the numerical solution, the differential equations were integrated along time. The integration scheme used was Newmark's β method, and the time step for the integration was Δt=0.005 sec. System damping was represented by Rayleigh damping and the damping ratio of 2.5 % in a first mode of free vibration of the system was used.

Addition to the calculation under the conditions mentioned above (Case 1), four calculations were conducted as listed in Table 2. The stabilising effect of the piles on the horizontal movement of abutment will be addressed in Case 2 using a model without piles. To gain further insight into the effects of interactions among river dyke, foundation ground and road embankment on the permanent deformation of the abutment, responses of the abutments isolated from the river dyke response and the downslope response of the road embankment were calculated in Cases 3 & 4, and response of the river dyke alone was calculated in Case 5. In Case 3, as three-dimensional interaction between the piles and soils has to be modelled properly even though the river dyke was not modelled, the

three-dimensional FE analysis was employed. However, for easy distinction of Case 3 from Case 1, the term 'quasi-2D' will be used to describe the analytical model for Case 3 in the subsequent text.

Limitations of the analysis are that (1) bridge(s) and associated bridge pier(s) are not modelled and (2) the abutment top could freely moves without restriction. Interaction between bridge(s) and the abutment is ignored, as our main concern is the interactions among the abutment, foundation ground, road embankment and river dyke. As a result of the limitations mentioned above, calculated deformation and/or vibration modes of the abutment could differ from those expected in a realistic bridge-foundation system.

3. ANALYSIS RESULTS AND DISCUSSION

3.1 Responses of abutment and surrounding ground

Figure 4 plots time histories of the horizontal displacement of the abutment top in Cases 1-4. In general the horizontal displacement of the abutment increased with shaking and two large fluctuations in the horizontal displacement time history coincided with the two large shocks in the input motion (see Fig. 3) for all the cases. Excess pore water pressure changes right below the abutment are shown in Fig. 5. In all the cases, at the first shock the excess pore water pressure changes showed steep dive while there were not such sudden changes at the second shock, and no full liquefaction was observed right below the abutment. Excess pore water pressure ratio contours at t=20sec (just after the second shock) for 3D analysis on the abutment without piles (Case 2) is shown in Fig. 6. It is noticed that the loose sand deposit just under the river dyke and road embankment was not fully liquefied while full liquefaction took place in the other area. Similar excess pore water pressure ratio distributions were obtained in the other cases.

As expected the permanent displacements of the piled abutment (Cases 1 & 3) were smaller than those of the abutment without piles (Cases 2 & 4) and were larger than those at the first large shock. The permanent displacement of the abutment without pile in 2D analysis (Case 4) was almost double of that in 3D (Case 2), while the permanent displacement of the piled abutment in quasi-2D analysis (Case 3) was more or less the same as that in 3D analysis (Cases 1). In both foundation conditions, differences in the accumulated excess pore water pressure underneath the abutment were not so large, as shown in Fig. 5.

Ground deformations around the abutment without piles (Cases 2 & 4) at t=30sec (when ground shaking almost ceases) are drawn in Fig. 7. Large shear deformation of the loose sand deposit under the abutment was observed in both cases. In the case of 3D analysis (Case 2), the road embankment showed relatively large settlement and marked settlement occurred just above the heel of the abutment base: This was probably due to the larger waterward displacement of the river dyke adjacent to the abutment (see ground deformation in the road level plan, the middle graph in Fig. 7). Similar plots for the piled abutment (Cases 1 & 3) are shown in Fig. 8. Only the remarkable difference in the deformation mode of the abutment with or without piles was the tilt of the abutment (no tilting for the former while remarkable for the latter). In this series of analyses, waterward movement of the river dyke was small and no typical lateral spreading like soil movement was observed, since the ground level behind the river dyke was relatively low compared to the river dyke height.

The above-mentioned calculation results reveal that assessment of the permanent dis-

placement of a non-piled abutment by two-dimensional FE analysis can overestimate the abutment response since in 2D analysis it's impossible to capture the three-dimensional movements of the river dyke and pore fluid, which can reduce the permanent displacement of the abutment. On the contrary, such marked difference in the permanent displacement cannot be seen for the piled abutment (Cases 1 & 3). In the following subsection, earth pressure acting on the abutments will be examined to clarify insensitivity of the piled abutment response to the 3D effects.

3.2 Earth pressure acting on abutment

Figure 9 shows time histories of sum of the effective earth pressure acting on the abutment back face (x=5m) at y=5m (horizontal force per unit width) and relative displacement of the abutment (x=−2.5m) to the backfill (x=7.5m, i.e., distance between two reference points is 10m), where positive value in the relative displacement represents elongation of the backfill. Before the arrival of the first shock, the earth pressure acting on the abutment back face was kept constant with gentle increase in the relative displacement between the abutment and backfill. At the first shock arrival, the earth pressure showed sharp spike in all the cases. When seismic performance of a piled road bridge abutment is assessed in accordance with the ductility design method adopted in the current specifications, this event is thought to be critical for the abutment. However, in all the cases, the horizontal displacements of the abutment when the maximum earth pressure acts on the abutment are not the maximum displacements throughout shaking (see Figs. 4 and 9). This evidence supports that the situation considered in the current specifications does not necessarily critical for the abutment and importance of consideration of the permanent deformation of surrounding soils for the abutment performance assessment. Behaviour of the abutment after the first shock is described in detail in the following.

After the arrival of the first shock, the earth pressures increased or decreased depending on the relative displacement between the abutment and backfill: In the cases on the abutment without piles (Cases 2 & 4), the relative displacement between the abutment and backfill increased with shaking, resulting in the small earth pressures that close to the active earth pressure, while the relative displacement was almost zero and the pressure acting on the abutment was kept constant at the higher level in the case on the pile abutment in the quasi-2D analysis (Case 3). The piled abutment in the 3D analysis (Case 1) showed intermediate behaviour. These changes in the earth pressure arise questions: (1) why the permanent displacements of the abutments without piles in 2D and 3D analyses differ vastly even though the abutments were subjected to almost the same earth pressure? (2) Why the permanent displacement of the piled abutment in quasi-2D analysis was almost identical with those in 3D analysis while there was large difference in the earth pressures acting on the abutment back face? Differences in the foundation soil resistance in 2D and 3D analyses may answer these questions.

Stress paths and stress--strain relations at the element right below the abutment without piles (Cases 2 & 4) are plotted in Fig. 10. Although the difference in the excess pore water pressure accumulation just below the abutment was not so large (see Fig. 5), the decrease in the mean effective stress, i.e., the increase in the excess pore water pressure, near the origin in the stress space made the limiting shear stress smaller, resulting in the smaller soil resistance and the larger shear strain as shown in Fig. 10. This difference in the excess pore water pressure at the non-piled abutment foundation is probably due to the

three-dimensional dissipation of the pore pressure. The calculation results suggest that such an effect is critical for stability of the abutment directly placed on the liquefiable soils.

Figure 11 plots distributions of the pile bending moment and the effective earth pressure acting on the pile in Cases 1 & 3. Bending moment distributions of the pile in 3D analysis (Case 1) were almost the same as those in the quasi-2D analysis (Case 3). The earth pressure distributions obtained tell us that the piles were subjected to the kinematic load induced by interaction between the liquefied soil and piles, which is not considered in the current ductility design method. Even though the earth pressure acting on the backfill-side pile in the quasi-2D analysis in the liquefiable layer was relatively larger than that on the other piles and those in 3D analysis, marked difference between the quasi-2D and 3D analyses in the kinematic loading couldn't be seen. In any case, (1) the shape of the distributions of the earth pressure acting on the pile and (2) the facts that marked difference in the earth pressure acting on the abutment less affects the piled abutment displacement confirm that the kinematic load as well as the loads considered in the current design method plays an important role in the assessment of the seismic performance of a piled abutment.

Earth pressure coefficient, K, contours at t=20sec in 3D analysis (Cases 1 & 2) are plotted in Fig. 12. K is the ratio of the effective horizontal stress to the vertical stress. As seen in this figure, the earth pressure coefficient in the bottom non-liquefiable layer just in front of the river-channel-side-piles (enclosed by circle) was higher in the case of the piled abutment and the width of the higher K region was limited to that of the abutment, while such a concentration could not be seen for the non-piled abutment case. This indicates that (1) the piles were laterally supported by the bottom non-liquefiable layer that may have been less affected by the three-dimensional dissipation of the excess pore water pressure and (2) the volume of soil that resisted against the load transferred by the piles was more or less the same both in quasi-2D and 3D analyses. As a result, the river dyke response did not affect much on the horizontal movement of the piled abutment and the seismic response of the piled abutment in the quasi-2D analysis was comparable to that in the 3D analysis.

In this series of analyses, waterward movement of the river dyke was small and no typical lateral spreading like soil movement was observed due to the lower ground level behind the river dyke. If the ground level behind the river dyke was high, remarkable difference in the permanent displacement of the abutment could be seen for the piled abutment as well.

4. SUMMARY

Dynamic three-dimensional finite element analyses on a bridge abutment constructed adjacent to a river dyke were performed considering liquefaction of foundation soils. Intention of the analyses was to demonstrate importance of consideration of pile kinematic loading induced by abutment backfill on assessment of seismic response of bridge abutment on liquefiable soils. In the course of numerical calculations, the following findings were also obtained: Numerical calculations on the non-piled abutment placed on the liquefiable ground revealed that the three-dimensional dissipation of the excess pore water pressure could alter the soil resistance under the abutment, resulting in smaller permanent displacement of the abutment in 3D analysis. On the other hand, such an effect was un-

remarkable for the piled abutment as the lateral load transferred by the piles was mainly supported by the bottom non-liquefiable layer (bearing stratum) that seemed nearly free from it in this study.

In this series of analyses, waterward movement of the river dyke was small and no typical lateral spreading like soil movement was observed, since the ground level behind the river dyke was relatively low compared to the river dyke height. If the ground level behind the river dyke was high, remarkable difference in the permanent displacement of the abutment could be seen for the piled abutment as well.

References

Hashiguchi, K. & Chen, Z.P. 1998. Elastoplastic constitutive equation of soils with the subloading surface and the rotational hardening. *International Journal for Numerical and Analytical Methods in Geomechanics*, Vol.22, 197-277.

Japan Road Association. 2002. Specifications for road bridges, Part V, Seismic Design, 333pp.

Shirato, M., Fukui, J. & Koseki, J. 2005. Current status of ductility design of abutment foundations against large earthquakes, *Soils and Foundations*, (submitted).

Table 1: Material parameters used.

(a) For soil layers

Parameter	Non-liquefiable layer (Dense sand deposit)	Liquefiable layer (Loose sand deposit)	Surface layer
G_s	2.65	2.68	2.68
e_0	0.65	0.85	0.85
κ	0.00054	0.00090	0.00090
λ	0.0072	0.019	0.019
ν	0.333	0.333	0.333
ϕ	41.3°	38°	38°
ϕ_d	27°	27°	27°
μ	0.5	1.0	0.0
ϕ_b	19.5°	19.5°	19.5°
b_r	2000	400	400
u_1	2	2	2
m_1	1	1	1
c	10	30	30
K_0	0.5	0.5	0.5
s_{ij0}	$0.7\sigma_{ij0}$	$0.2\sigma_{ij0}$	$0.2\sigma_{ij0}$
OCR	16	2	2
k (m/s)	5×10^{-4}	5×10^{-4}	–

(b) For piled abutment

Parameter	ρ (Mg/m^3)	EI (GN.m^2)	EA (GN)	E (GPa)	ν
Pile	2.5	4.2	79	–	–
Abutment	2.5	–	–	21	0.3

Table 2: Analysis conditions.

Case	Abutment	River dyke	
1	w/ piles	O	– (3D analysis)
2	w/o piles	O	– (3D analysis)
3	w/ piles	X	Width of abutment is assumed infinite (Like long retaining wall, 3D analysis).
4	w/o piles	X	Width of abutment is assumed infinite (2D analysis).
5	X	O	River dyke (2D analysis).

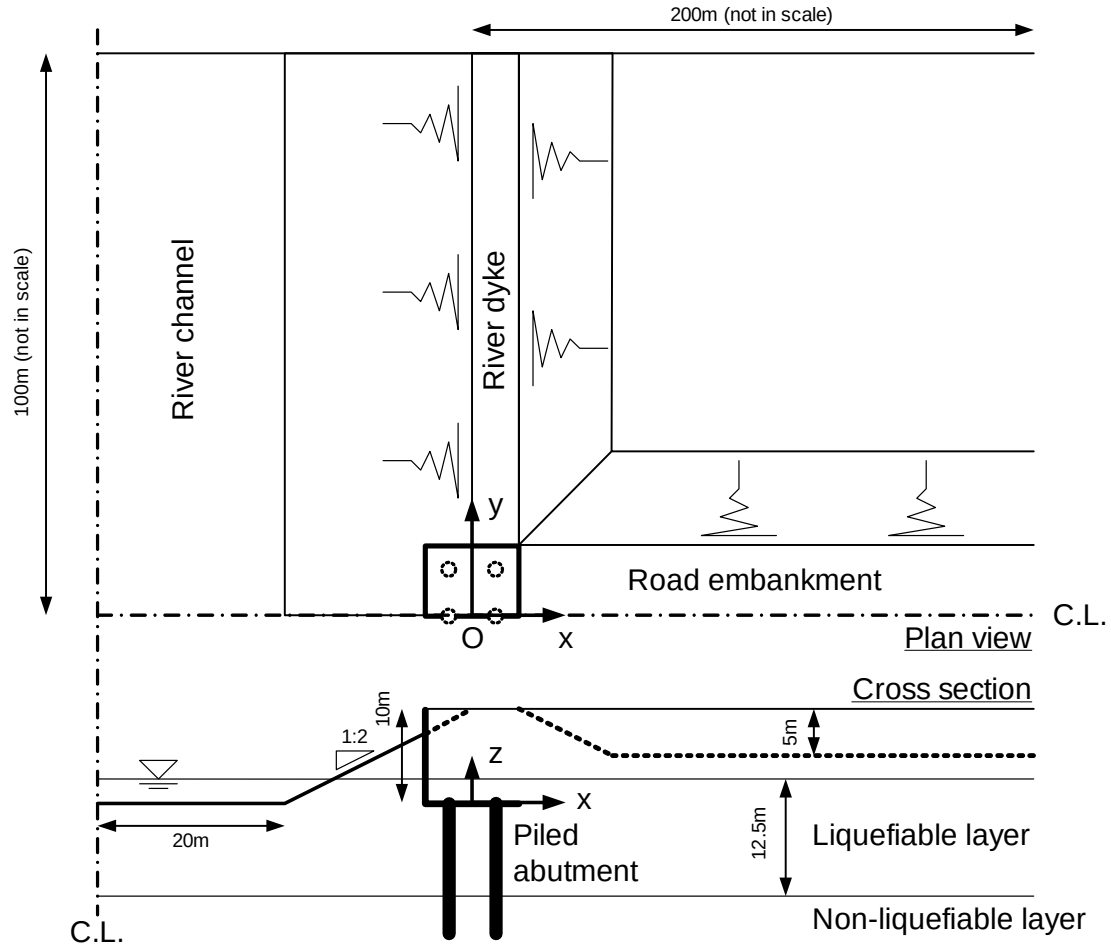

Figure 1: Plan view and cross section of target abutment.

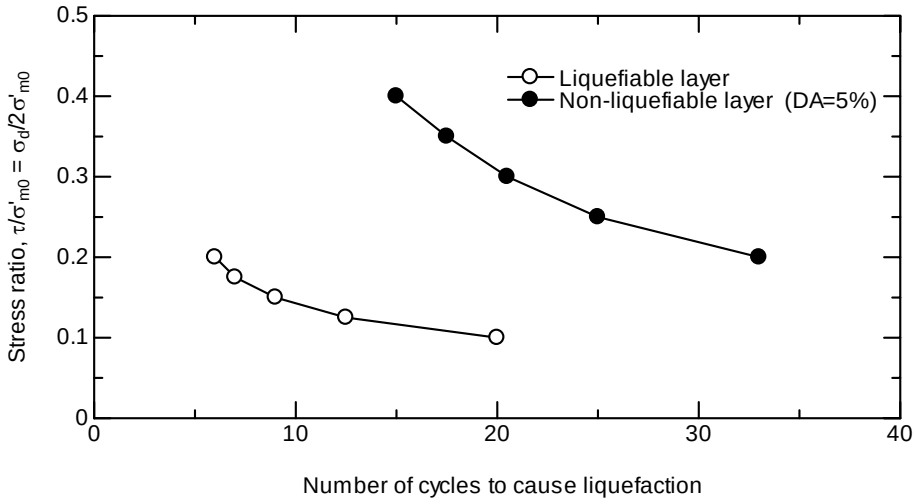

Figure 2: Relationship between cyclic stress ratio and number of cycles to cause liquefaction.

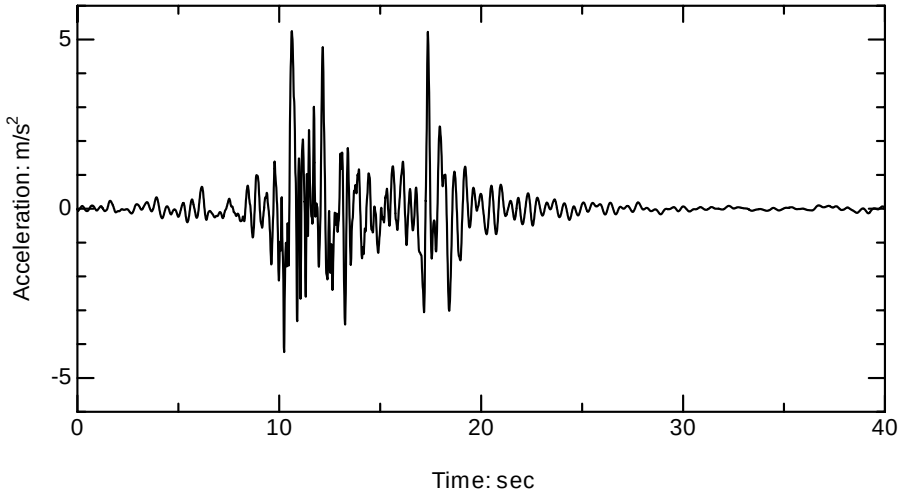

Figure 3: Time history of input motion.

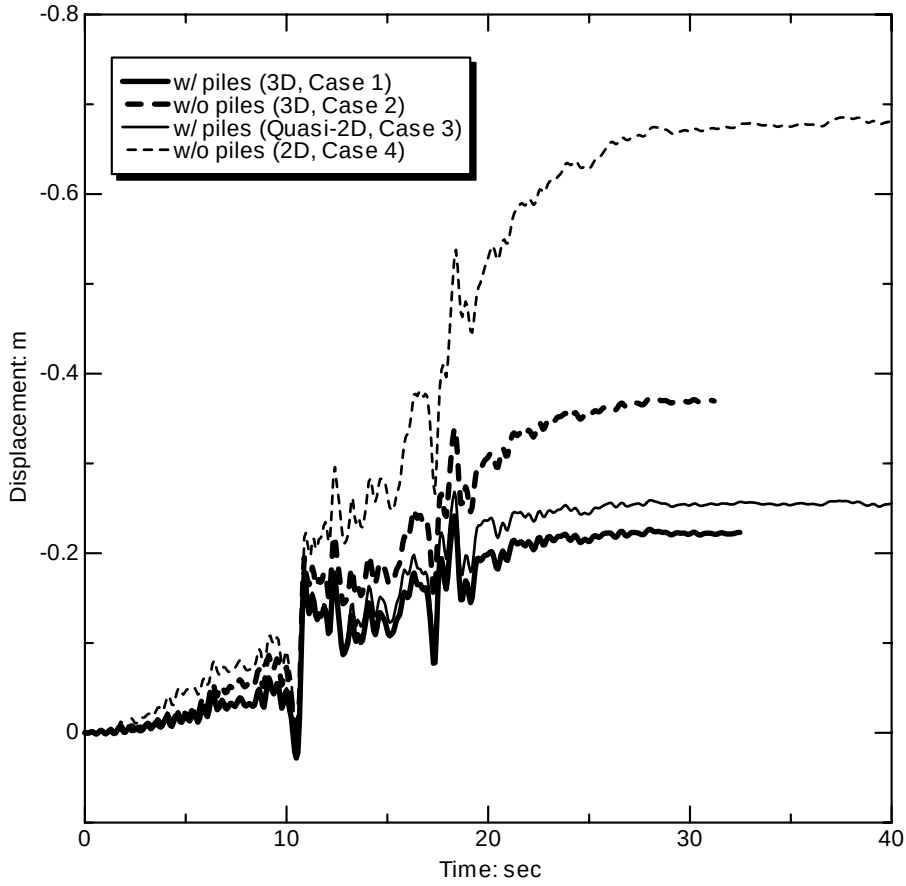

Figure 4: Time histories of horizontal displacement of abutment top (Cases 1-4).

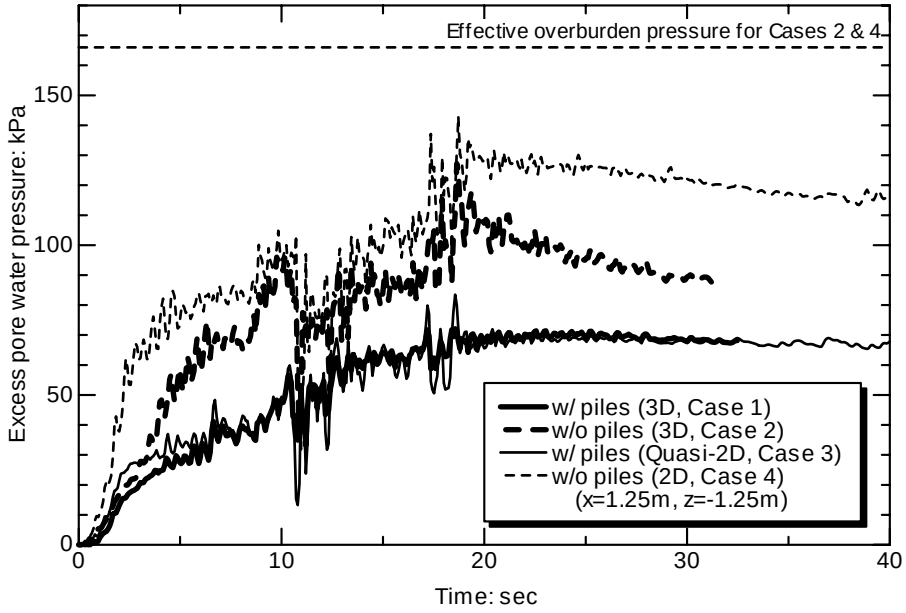

Figure 5: Time histories of excess pore water pressure right below abutment (Cases 1-4).

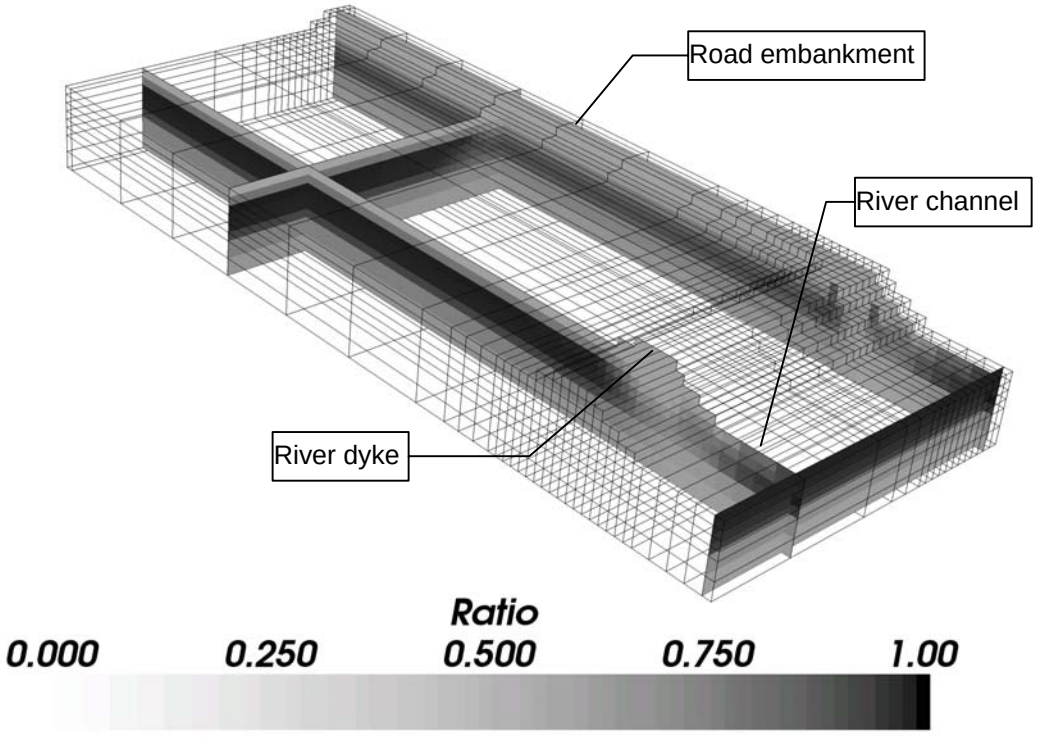

Figure 6: Excess pore water pressure ratio contours at *t*=20sec (Case 2)

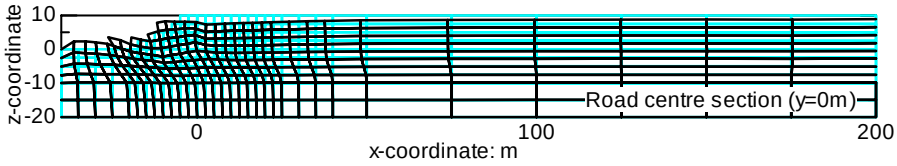

(a) Ground deformation in 2D analysis (Case 4)

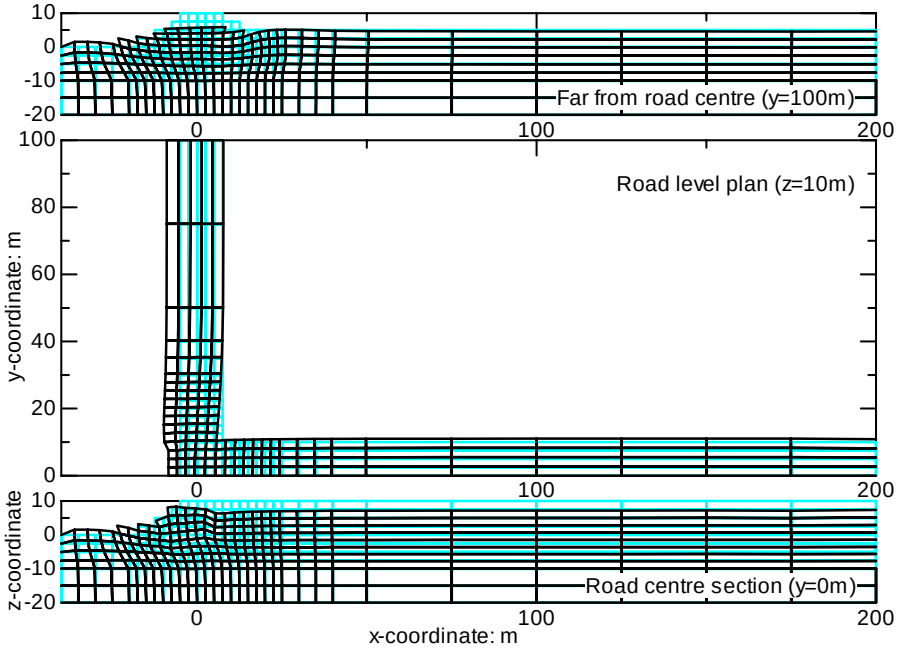

(b) Ground deformation in 3D analysis (Case 2)

Figure 7: Ground deformations around abutment without piles, where displacement scale is magnified by a factor of ten (Cases 2 & 4 at *t*=30sec)

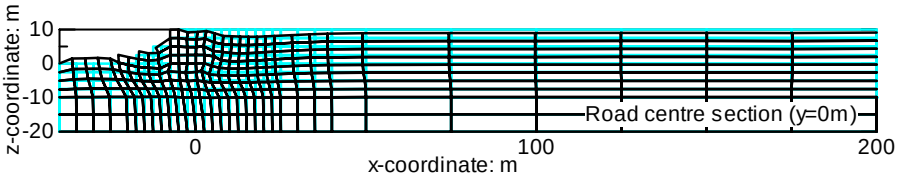

(a) Ground deformation in quasi-2D analysis (Case 3)

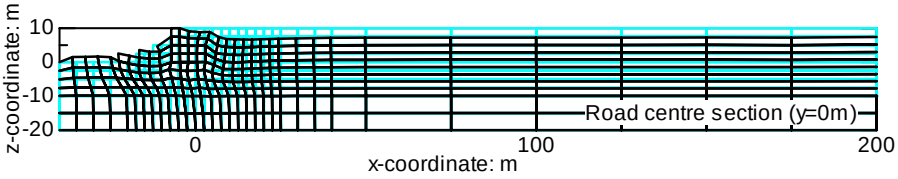

(b) Ground deformation in 3D analysis (Case 1)

Figure 8: Ground deformations around piled abutment, where displacement scale is magnified by a factor of ten (Cases 1 & 3 at *t*=30sec)

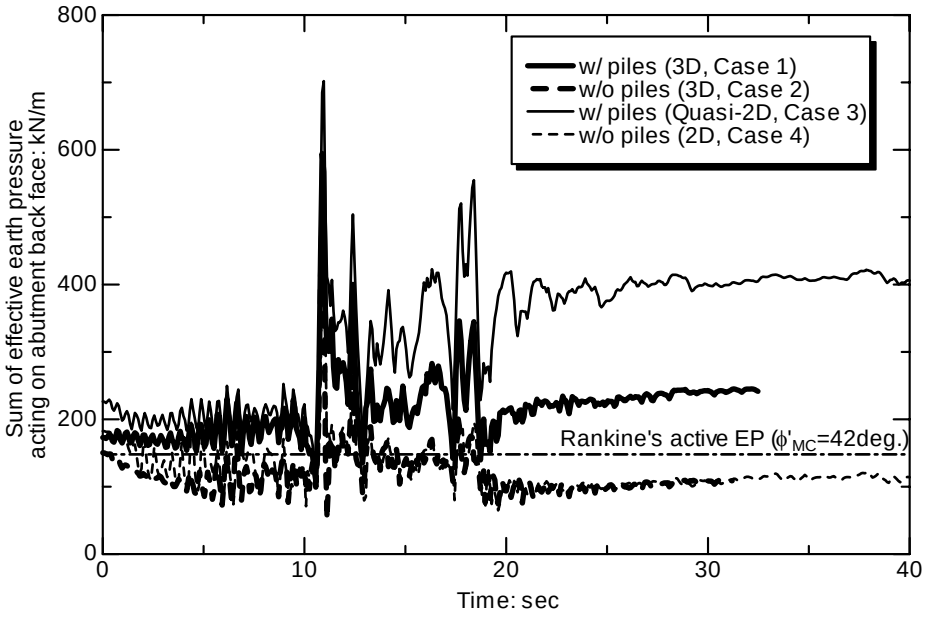

(a) Changes of sum of effective earth pressure acting on abutment back face

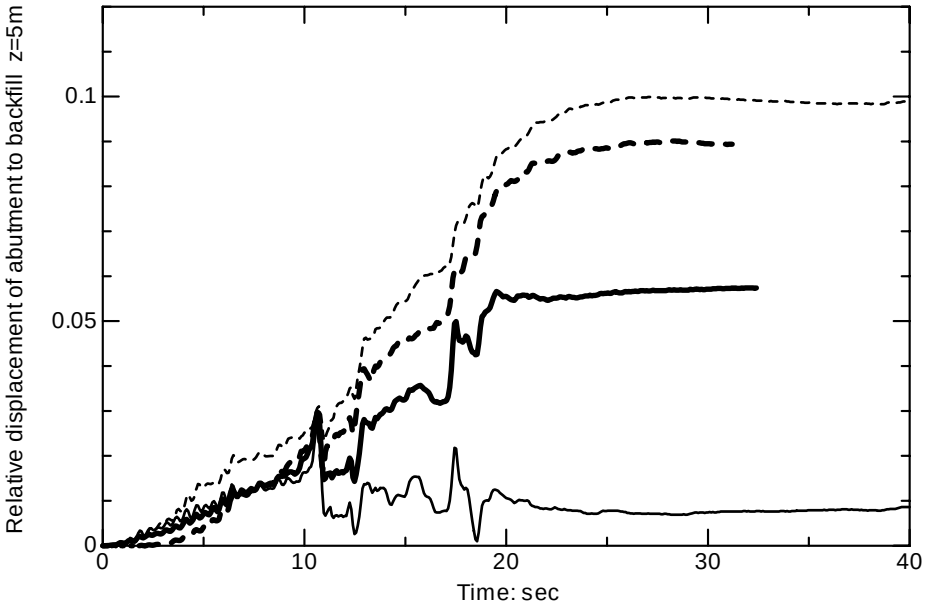

(b) Changes of relative displacement of abutment to backfill at z=5m

Figure 9: Time histories of (a) sum of effective earth pressure acting on abutment back face and (b) relative displacement of abutment to backfill (distance between two reference points is 10m), where positive value in relative displacement represents elongation of backfill.

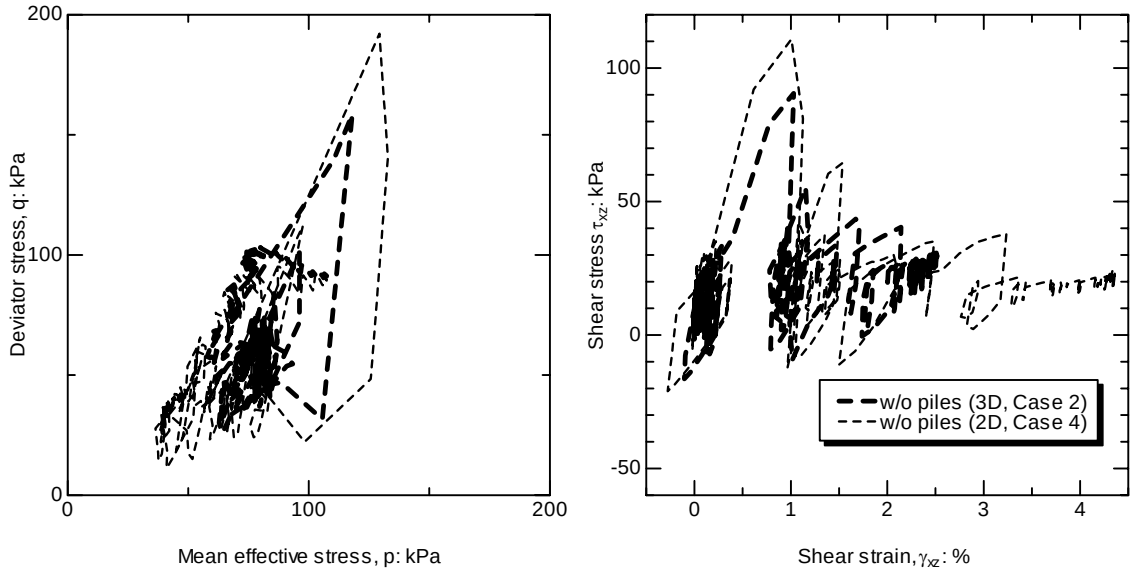

Figure 10: Stress paths (left) and stress--strain relations (right) at element right below abutment without piles (Cases 2 & 4).

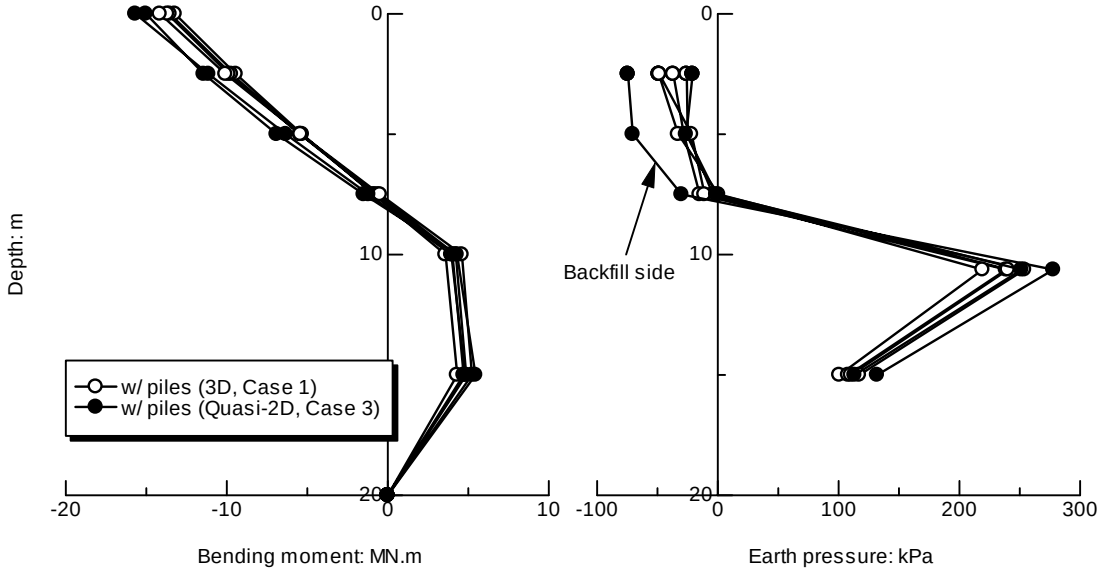

Figure 11: Distributions of pile bending moment (left) and effective earth pressure acting on pile (right) in Cases 1 & 3.

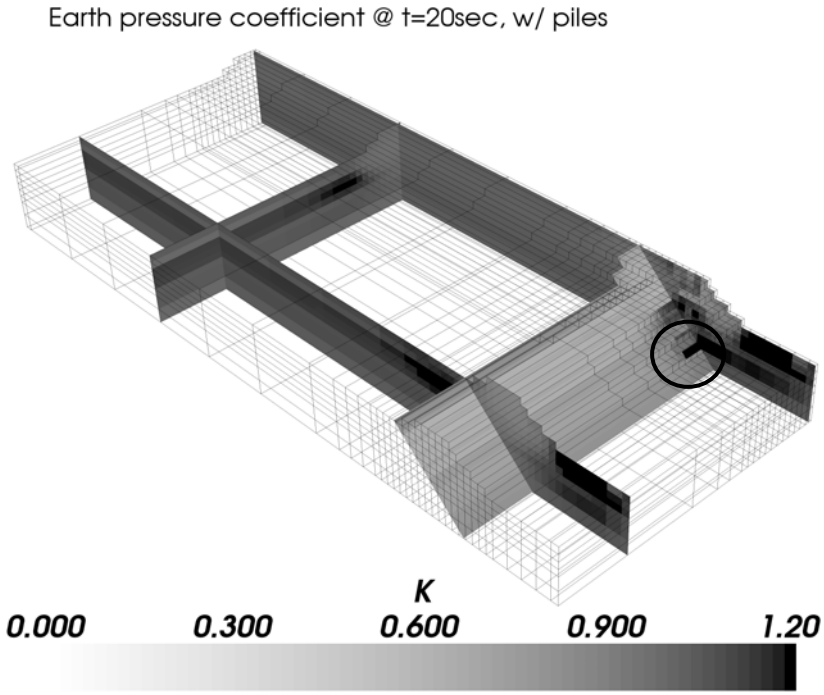

(a) With piles (Case 1)

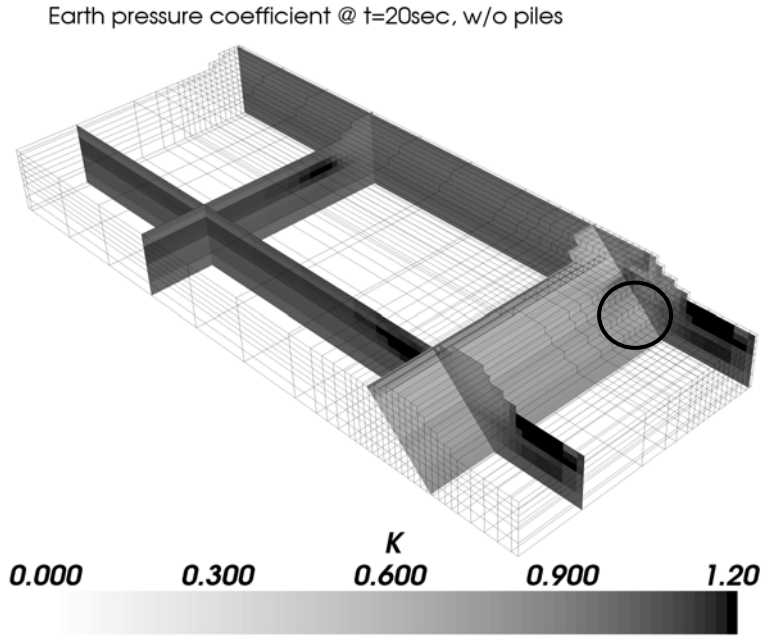

(b) Without piles (Case 2)

Figure 12: Earth pressure coefficient contours at *t*=20sec in (a) Case 1 & (b) Case 2.